Single-event spectroscopy and unravelling kinetics of covalent domains based on cyclobutane mechanophores

Brandon H. Bowser^{1,2‡}, Shu Wang^{1,2‡}, Tatiana B. Kouznetsova^{1,2}, Haley K. Beech^{1,3}, Bradley D. Olsen^{1,3,*}, Michael Rubinstein^{1,2,4,5*} and Stephen L. Craig^{1,2,*}

¹NSF Center for the Chemistry of Molecularly Optimized Networks; ²Department of Chemistry, Duke University, Durham, North Carolina 27708, United States; ³Department of Chemical Engineering, Massachusetts Institute of Technology, Cambridge, Massachusetts 02139, United States; ⁴Departments of Physics, Mechanical Engineering and Materials Science, and Biomedical Engineering, Duke University, Durham, North Carolina 27708, United States; ⁵World Premier Institute for Chemical Reaction Design and Discovery, Hokkaido University, Sapporo, JAPAN.

Supporting Information Placeholder

ABSTRACT: Mechanochemical reactions that lead to an increase in polymer contour length have the potential to serve as covalent synthetic mimics of the mechanical unfolding of noncovalent "stored length" domains in structural proteins. Here we report the force-dependent kinetics of stored length release in a family of covalent domain polymers based on cis-1,2-substituted cyclobutane mechanophores. The stored length is determined by the size (n) of a fused ring in an [n.2.0] bicyclic architecture, and it can be made sufficiently large (> 3 nm per event) that individual unravelling events are resolved in both constant-velocity and constant-force single-molecule force spectroscopy (SMFS) experiments. Replacing a methylene in the pulling attachment with a phenyl group drops the force necessary to achieve rate constants of 1 s⁻¹ from ca. 1970 pN (dialkyl handles) to 630 pN (diaryl handles), and the substituent effect is attributed to a combination of electronic stabilization and mechanical leverage effects. In contrast, the kinetics are negligibly perturbed by changes in the amount of stored length. The independent control of unravelling force and extension holds promise as a probe of molecular behavior in polymer networks and for optimizing the behaviors of materials made from covalent domain polymers.

Introduction.

Biological systems have a variety of mechanisms for productively responding to an applied mechanical load. The muscle protein titin, for example, releases elastic energy via the unfolding of structural domains, ¹⁻⁸ and the resulting mechanics couple to the activity of actin and myosin to build muscle strength in response to repeated load bearing. The folded domains of titin and similar proteins (**Figure 1a**) act as sources of "stored"

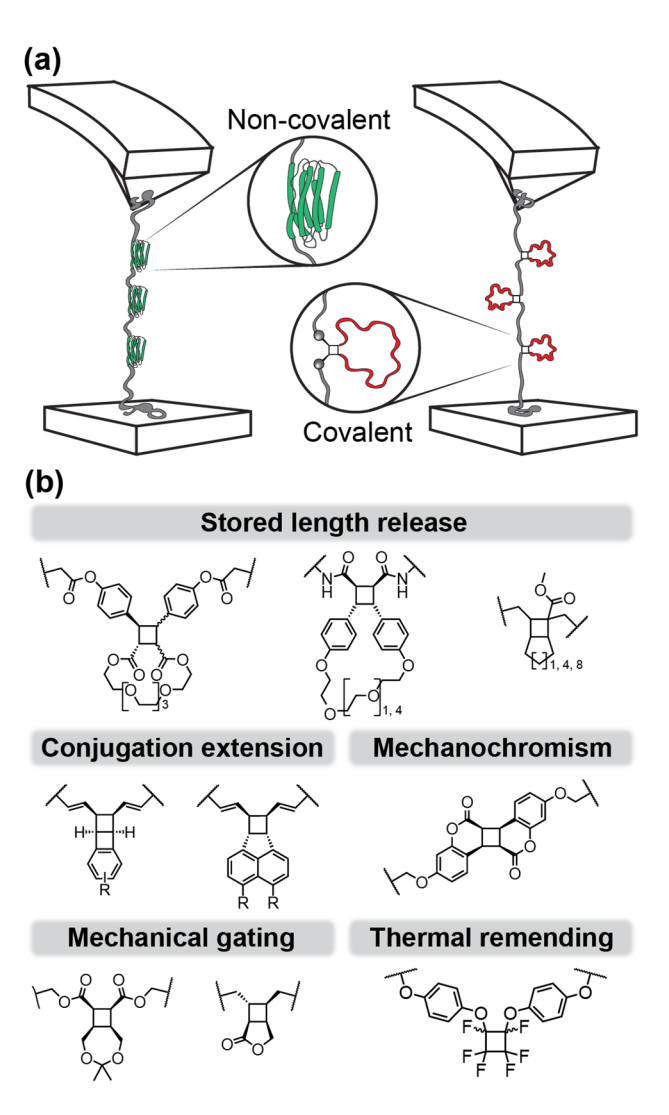


Figure 1. a) Cartoon representation of SMFS of non-covalent (left) and covalent (right) domain polymers. b) Reported applications of cyclobutane-based mechanophores.

length" that are unveiled when a force is applied, leading to an extension in the overall length of the protein. Similar strategies have recently been brought into synthetic polymers. 9-10 Chung et al. designed a biomimetic polymer in which individual repeats comprise large macrocycles that are contracted by hydrogen-bonding interactions that span the loop interior. 11 Using single-molecule force spectroscopy (SMFS), they were able to observe the kinetics of individual unfolding and re-folding events that are responsible for mechanical property enhancements in bulk materials.

The energy dissipation achieved by domain unfolding can be greatly enhanced by stored length that is released through the scission of covalent, rather than noncovalent, interactions (**Figure 1a**). 12-17 Because covalent bonds require higher forces for rupture, these "covalent domain polymers" (CDPs) are capable of single-strand toughness that far exceeds that of conventional synthetic polymers. Within a polymer network, increased singlechain toughness could also contribute to changes in other bulk material properties, such as the fracture toughness of network elastomers. 18 The design, synthesis, and characterization of CDPs is therefore of growing interest, and recent years have seen the emergence of covalent stress-responsive monomers (mechanophores) that unveil stored length through force-coupled covalent reactions in highly stretched polymer chains. A promising class of mechanophores in this regard involves cyclobutanes (Figure 1b) that are fused to other cyclic, covalent domains. 12-14,16-17,19-26 Stress is typically applied to one side of the cyclobutane via the polymer backbone, causing the cyclobutane to ring-open through a [2+2] cycloreversion, releasing the length stored in the fused ring on the other side of the cyclobutane "gate." Whereas many mechanophores, such as those based on the ring-opening reactions of gem-dihalocyclopropanes and cyclobutenes, ²⁷⁻²⁸ involve modest (< 1 nm) changes in polymer contour length, the architecture of fused cyclobutanes provides access to greater length changes that can, in rare examples, be individually resolved in single molecule force spectroscopy experiments. Pill et al., for example, were able to observe the ring-opening of a single cyclobutane mechanophore embedded in an end-tethered polymer, 19 and more recently Weng and Boulatov have resolved individual ring-opening events within polymers that contain multiple cyclobutane repeats. 13-14 In one of the latter examples, the polymer contour length more than doubles as a result of the complete opening of all mechanophores.¹³

The impact of force-coupled cyclobutane cycloreversion kinetics have also recently come to the fore in the

context of polymer network fracture. Poly(ethylene glycol) (PEG) gels were synthesized through the end-linking of azide-terminated tetra-arm PEG ($M_n = 5 \text{ kDa}$) with bis-alkyne linkers. When the bis-alkyne includes either a cis-diaryl or cis-dialkyl linked cyclobutane "weak link" mechanophore, the tearing energy of the gels is substantially reduced relative to that of a control network.²⁹ In addition, the *cis*-diaryl cyclobutane gel is much more easily torn than the cis-dialkyl analog. The difference in fracture energies is correlated with qualitative characterization of the force-coupled scission kinetics of the mechanophores observed in single-molecule force spectroscopy experiments, implicating local resonance stabilization of a diradical transition state in the cycloreversion of CB4 as a key determinant of the relative ease with which its network is torn. Together, these growing uses of cyclobutane mechanophores in polymer networks motivate a more detailed characterization of their force-coupled reactivity.

Herein we explore structure-activity relationships in the mechanochemical reactivity of a subset of fused ring cyclobutanes that are built via a modular approach, reminiscent of the work of Weng and Boulatov (Figure 2). ¹³⁻¹⁴ The modularity allows the force-coupled kinetics and the amount of stored length that is released upon activation to be tuned independently. When the stored length exceeds 3 nm per mechanophore, we are able to resolve individual ring-opening events via SMFS under both constant-velocity and constant-force conditions. The resolution of individual events allows the constantvelocity data to be converted into the equivalent forceclamping data through a binning strategy. This analysis unites the two data sets and expands the dynamic range of the force-coupled kinetics experiments, allowing a fuller picture of the mechanochemical cycloreversion reaction to be achieved. We find that the size of the fused macrocycle does not substantially influence the force-coupled reactivity, whereas the chemical structure of the pulling attachments has a profound effect. In particular, the use of 1,2-cis-diphenyl substituents as pulling attachments provides a mechanical advantage relative to dialkyl analogs. That mechanical advantage works in concert with electronic stabilization of the force-coupled transition state for cycloreversion, which combine to substantially reduce the force required for activation for the same timescale regime (ms to min). The characterized force dependencies and structural modularity of the mechanophores provide a quantitative foundation for the use of these cyclobutane mechanophores in general, and their CDPs in particular, in forceresponsive polymers and polymer networks.

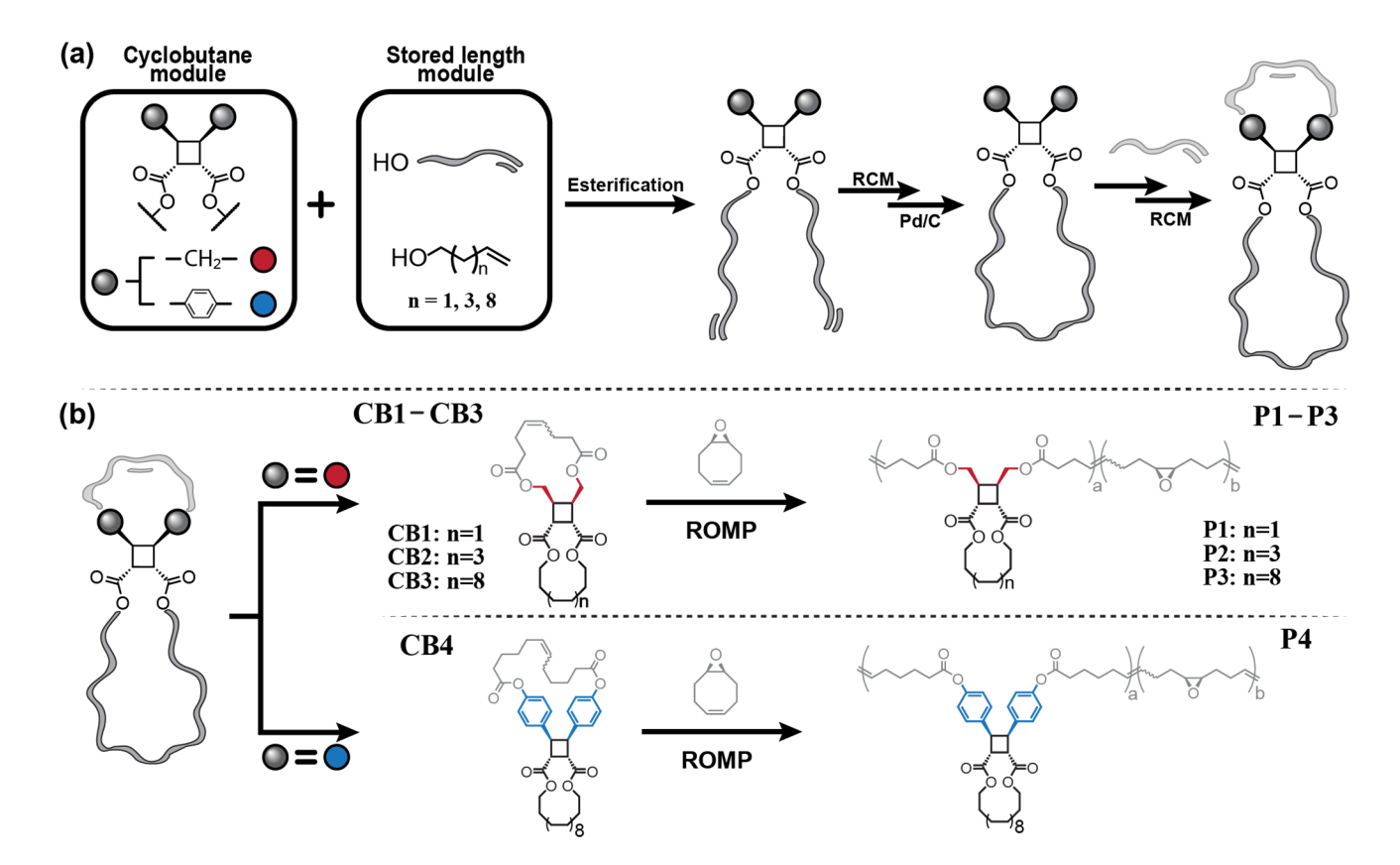


Figure 2. a) Cartoon of monomer synthesis, highlighting the modular approach for incorporating stored length. b) Chemical structures of monomers and ROMP-derived copolymers.

Experimental.

Monomer and polymer synthesis. The mechanophores and polymers studied are shown in Figure 2. Cyclobutane monomers CB1-CB3 have the same mechanophore "gate" structure, only differing in the size of the fused ring. Monomer CB4 has the same fused ring as CB3, but differs from CB1-CB3 in that the pulling attachments are phenyl rings as opposed to methylenes. Similar phenyl-substituted cyclobutane mechanophores have been reported previously,¹³ but we note that the synthetic strategy employed here provides greater stereochemical fidelity than the previous method, which in turn provides greater control over single chain mechanochemical properties. All monomers were prepared using a modular approach, wherein the size of the fused ring is ultimately determined by the length of the alcohol used during the first esterification reaction (Figure 2). Once these linkers with terminal alkenes are attached to the cyclobutane core, ring-closing metathesis (RCM) closes the macrocycle that serves as the source of stored length. The alkene resulting from RCM is then reduced via a palladium-catalyzed hydrogenation so that "handle side" of the cyclobutane core can be functionalized with another cyclic alkene. Rather than being used for stored length, this cyclic alkene is copolymerized with epoxy-COD via entropy-driven ring-opening metathesis polymerization (ED-ROMP), generating high molecular weight (MW) polymers that contain multiple cyclobutane repeats (P1-P4).³⁰ The epoxide comonomer is mechanically inert and has been shown to increase the adhesion force between the polymer and the tip of the atomic force microscope (AFM) cantilever.³¹ Percent monomer incorporation was determined by ¹H NMR. Molecular weights were determined by gel permeation chromatography equipped with a multi-angle light scattering detector (GPC-MALS).

Single molecule force spectroscopy. Pulling experiments were conducted using a homemade AFM at ambient temperature in toluene, using a similar procedure to that described previously. 30,32-34 Force curves used for analysis were obtained with rectangular-shaped cantilevers (205 μm x 15 μm, nominal tip radius ~2 nm, nominal spring constant k ~ 0.02 N/m, frequency ~ 15 kHz). Multiple probes of the same type were used throughout the course of the experiments. The spring constant of each cantilever was calibrated in air, using the thermal noise method, based on the energy equipartition theorem as described previously.³⁵ Cantilever tips were prepared by soaking in piranha solution for ~15 min at room temperature. Silicon surfaces were prepared by soaking ~30 min in hot piranha solution, followed by washing with DI-water and drying under a stream of nitrogen. The surface and cantilever were then placed in a UVO cleaner for 15 min. After ozonolysis, the cantilever was mounted into the AFM, and ~20 μL of a ~0.1

mg/mL polymer solution was added to the silicon surface and allowed to dry.

Measurements were carried out in a fluid cell with scanning set for a series of constant velocity approaching/retracting cycles. To collect "constant-force" data, cantilever deflection was monitored during each retraction cycle. Once the cantilever deflection reached a threshold value (set here to 200 pN), the system was switched to the force-control mode to achieve a desired set point force value for the constant force measurement. This active control of force was maintained for a set period of time (10-30 sec), after which the force-control mode was switched off and constant velocity retraction resumed to finish the pulling cycle. During acquisition, data were filtered at 500 Hz and collected in dSPACE and Matlab.

Data analysis. Matlab was used to analyze changes in polymer contour length associated with mechanophore activation for both constant-velocity and constant-force experiments. For constant-velocity experiments, an extended freely-jointed chain (EFJC) model was used to fit the force curves before and after the transition region (Figure S1-4), allowing for the determination of the initial polymer contour length before any mechanophores react (L_1) and the final contour length after all covalent domains have unraveled (L_2) . For **P3** and P4, the same approach was used to fit individual domain unfolding events within a single force curve, in order to determine the contour length before (l_1) and after (l_2) a single activation. For the purposes of this analysis, we only measured the change in contour length for a given event if we could resolve and successfully fit two adjacent peaks (Figure S5-6). For constant-force data, the force-coupled length before (l_1) and after (l_2) each rupture event is determined directly from steps in the distance vs. time curves.

Modeling. The expected change in contour length was calculated by employing a relaxed potential energy scan across a range of fixed end-to-end distances, similar to the well-established CoGEF methodology (Constrained Geometry simulates External Force) but without attempting to simulate the actual reactivity. 31-32,36-39 Here, the approach is used only to calculate monomer contour lengths as a function of an applied force. We use the contour lengths found at relatively high forces (e.g., forces relevant in SMFS experiments) to extrapolate to a force-free contour length, in a computational process that is analogous to the extrapolation of a force-free contour length from the high-force extensional behavior of chains in the SMFS experiments. Because we are only interested in the relative contour lengths before and after unravelling, these calculations can be done at a low level of theory.

Briefly, the equilibrium conformers of monomers **CB3** and **CB4**, in both their ring-closed and ring-opened

states, were minimized at either the molecular mechanics or semi-empirical levels of theory. The end-to-end distance of a monomer was constrained until the bonding geometries were noticeably distorted. Energy as a function of displacement was then obtained by shortening the constraint in 0.1 Å increments. The incremental change in energy $(E_n - E_{n-1})$ vs. change in distance $(d_n - d_{n-1})$ was taken as the force at the midpoint of the increment, and the resulting force vs. displacement curve was extrapolated to zero force to give a force-free contour length (**Figure S15-18**).

Results and Discussion.

The ED-ROMP methodology yielded high MW copolymers that contain multiple fused-ring cyclobutanes. Polymer molecular weight (GPC-MALS) and monomer content (¹H NMR) is summarized in **Table 1**. For polymers **P3** and **P4**, multiple polymers with varying composition and molecular weight were synthesized and characterized.

Table 1. Summary characterization data of polymers employed in this study. Molecular weights are determined by GPC-MALS and monomer content by ¹H NMR.

Polymer	M _n (kDa)	M _w (kDa)	Đ	% CB	% epoxide
P1	245	329	1.3	27	73
P ₂	226	356	1.6	20	8o
P3-a	370	474	1.3	35	65
P ₃ -b	266	425	1.6	10	90
P3-c	219	268	1.2	33	67
P ₃ -d	289	449	1.6	40	6o
P4-a	171	313	1.8	32	68
P4-b	139	160	1.2	87	13

Representative force vs. separation curves obtained from constant-velocity (CV) SMFS for each polymer are shown in **Figure 3a-b**. As a polymer is pulled, the force along its backbone increases, and the probability of mechanophore unravelling increases with it. The force continues to increase until the rate at which stored length is released becomes competitive with the rate at which the polymer is being stretched (300 nm/s). The competition between these two processes results in a plateau in the force-extension curve, where the overall force remains relatively constant as the contour length of the polymer increases.

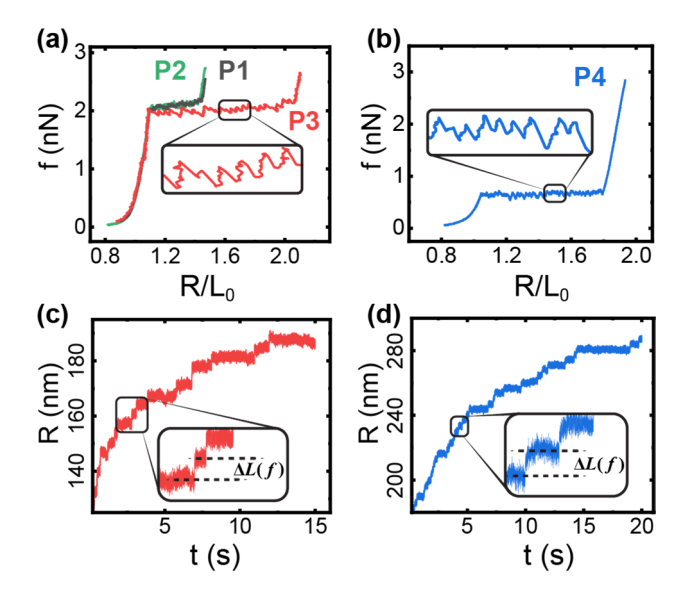


Figure 3. a-b) Representative normalized force vs. separation curves for polymers P1-P3 (a) and P4 (b), obtained by constant-velocity SMFS. Insets highlight the sawtooth pattern observed in the plateau regions for **P3** and **P4**. c-d) Representative distance vs. time curves for **P3** at 1860 pN (c) and **P4** at 600 pN (d), obtained by constant-force SMFS. Insets highlight the staircase pattern and extraction of stored length release per activation.

Representative distance vs. time curves obtained from constant-force SMFS, also known as force-clamp (FC) spectroscopy, are shown in **Figure 3c-d** for **P3** and **P4**. These polymers were each clamped for ~10-30 s at several different forces (~1800 pN for **P3** and ~700 pN for **P4**) that are just below the plateau forces observed in the respective constant-velocity experiments (**Figure 3a-b**). If held at a sufficiently high force for enough time, the CB monomers react and release slack, leading to an increase in polymer contour length. Thus, the "plateaus" in the FC data represent how much time the polymer spends at a given degree of unravelling before another unravelling event occurs (which is indicated by a sudden jump from one plateau to the next).

Domain size. We first analyze the amount of slack that is released (measured by SMFS) for a typical unravelling event and correlate slack release to the size of the fused covalent domain. As seen in a magnified section of the plateau region for P3 and P4 (Figure 3a-b), the plateau comprises a series of sawtooth features that are ascribed to the unravelling of individual covalent domains. These features are detectable, but not as easily resolved, in P1 and P2 (Figure S1-3), which contain smaller fused domains than P3 and P4. The observation that the ability to resolve the "teeth" of the plateau depends on domain size is evidence that each tooth likely corresponds to individual events. We therefore limit the domain size analyses and single event-based extraction of force-dependent kinetics to polymers P3 and P4.

For **P3** and **P4**, each "tooth" of the sawtooth pattern is fit with an EFJC model using the Kuhn length and segment elasticity parameters obtained on nascent polymer, as described above, in order to determine the change in contour length for individual ring-opening events. The frequency histogram of the aggregate data (0.2 nm bin size) was fit to a Gaussian distribution (**Figure 4a-b**), and the average change in contour length per event was found to be 3.16 ± 0.21 nm and 3.13 ± 0.35 nm for **P3** and **P4**, respectively. Uncertainties correspond to the standard deviation of the Gaussian fit. These experimental values are consistent with values of 3.13 nm and 3.40 nm obtained from calculations on **P3** and **P4**, respectively (**Figure 4e-f**).

A similar analysis is applied to the staircase pattern of the corresponding FC curves (**Figure 3c-d**), where the transition between steps corresponds to the unravelling of individual covalent domains. The distribution of step sizes (**Figure 4c-d**) is again characterized and used to determine the average change in length per single event. Because the force range explored in FC experiments is narrow (less than 100 pN per polymer), we aggregate data across all pulls. Fitting the aggregate data (0.2 nm

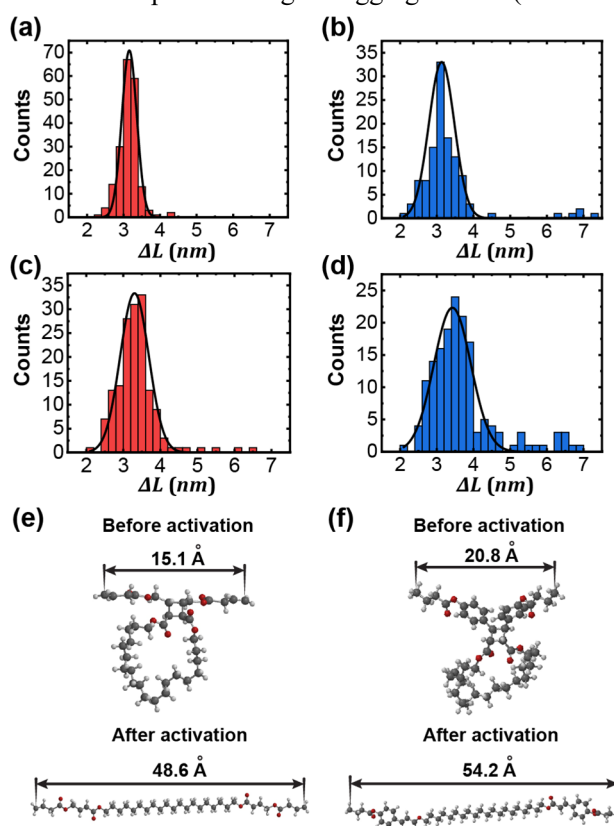


Figure 4. a-d) Histograms of changes in polymer contour length per detected activation, obtained from constant-velocity (a-b) and constant-force (c-d) experiments for polymers P3 (a,c) and P4 (b,d). All bin sizes are 0.2 nm and the histograms were fit with a Gaussian distribution (black

curve). e-f) Representative structures of mechanophore repeats and their associated end-to-end distances in both their nascent and fully unraveled states, obtained from CoGEF calculations.

bin size) with a Gaussian distribution yields average values of 3.30 ± 0.39 nm for **P3** and 3.42 ± 0.51 nm for **P4**, which are in agreement with those extracted from constant-velocity experiments and those predicted by the CoGEF calculations for a single activation event. The uncertainty in the extrapolations precludes a deep comparison of the extensions between the two experiments. We note, however, that it makes sense for the changes in contour length extracted from the constant velocity and FC measurements to differ, because the FC analysis obtains the change in contour length under an applied force, whereas the constant velocity curves are extrapolated back to zero force.

Force-coupled kinetics. Before discussing the extraction of force-dependent kinetics from the data, we make an initial, qualitative observation about the kinetics by comparing the transition forces (the force at which the plateau occurs) for P1-P4 that are observed in the constant-velocity experiments. For P1-P3, where the only difference in the monomer structures is the size of the fused ring, we see that the transitions in the force curves overlay (Figure 3a), indicating that within the range of ring sizes studied here, a change in the size of the fused macrocycle does not lead to substantial changes in the force-coupled reactivity of the cyclobutane, and that the amount of stored length can be treated as a parameter that can be tuned independently within this class of mechanophores.

As seen in comparing Figure 3a to Figure 3b, however, the attachments (phenyl vs. alkyl) through which the polymer is coupled to the cyclobutene have a major influence on the transition force. The transition force of **P4** is \sim 1300 pN lower than that of **P1-P3**. Boulatov and coworkers have recently shown experimentally that the stereochemistry of phenyl pulling attachments can greatly alter the force-coupled reactivity of cyclobutane. 13 but we are not aware of previous experimental comparisons of different handles with the same stereochemistry (here, "cis-pulling") in cyclobutanes. The observed difference in reactivity between phenyl and alkyl pulling attachments can be partially explained by differences in the ability of the substituent to stabilize the radicals that are presumably generated from the first bondbreaking event; 16,23 the CH bond dissociation energy of a phenyl-substituted methylene, CH(CH₃)(C₆H₅), is ~13 kcal/mol lower than the CH bond of the analogous methyl-substituted methylene, CH(CH₃)₂.⁴⁰ In addition to this electronic effect, we also considered that the phenyl substituents might provide better mechanical leverage compared to the alkyl attachments, as demonstrated in other mechanophores. 31,38 Such mechanical lever-arm effects would also influence the force-coupled kinetics.

Differences in mechanical leverage correspond to differences in force sensitivity – how relative rate changes as a function of force. The force-dependent kinetics were extracted via two approaches: (i) survival statistics that take into account the changing force of the constant velocity experiments, and (ii) survival statistics in the constant force experiments. The latter approach, based on FC spectroscopy, is often used to study protein unfolding, $^{6,41-42}$ but it has been employed to study covalent mechanophores in only rare instances. 34,39 We fit the distance vs. time curves with a single exponential decay function to provide k(f) at several different forces for both **P3** and **P4**. The various rate constants are plotted as a function of the force in **Figure 5** ("X" symbols).

Additional kinetic data (**Figure 5**, circles) were extracted from CV force-extension curves for **P3** and **P4** using a bin-based approach previously developed by our group and then independently by Osterhelt. ⁴³⁻⁴⁴ Full details are provided in the Supporting Information, but, briefly, Matlab is used to count the total time spent by cyclobutane mechanophores within a given force range t(f), where f here refers to all forces that fall within a range (typically 20-50 pN). The residence time t(f) is determined by multiplying the number of digital data points found within a given force range by the acquisition time and the number of cyclobutanes in the loaded

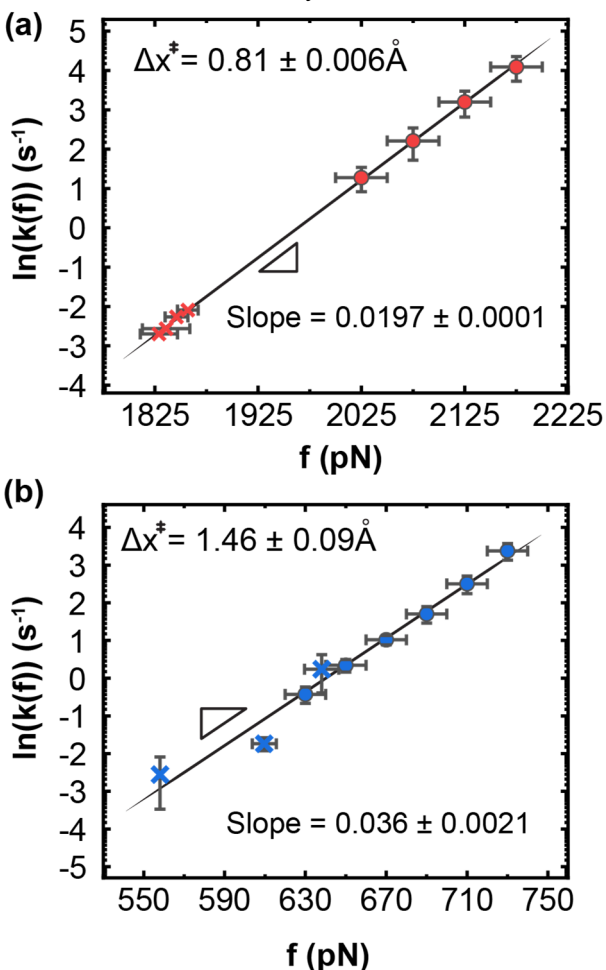


Figure 5. Rate vs. force plots for polymers P3 (a) and P4 (b). " \mathbf{x} " symbols correspond to data from constant-force experiments and circles correspond to data from constant-velocity experiments. Slopes of linear fits of the combined data are reported, along with the mechanochemical coupling parameter, Δx^{\ddagger} , obtained from eq. 1.

polymer strand that are still intact at that time each data point is recorded. The number of bond ruptures in a given force range, N(f), is counted using Matlab's builtin *findpeaks* function. Adjustments are made to account for the fact that some single events are unable to be resolved, and double or triple events (< 25%) are determined based on the measured change in strand length and accounted for in the analysis (Figure S7-9). Note that t(f) and N(f) are usually taken from multiple curves with different numbers of rupture events, since a single curve might not have enough rupture events for analysis. We then total t(f) and N(f) across several pulls to obtain a group of t(f) and N(f) data with more than 100 rupture events, (Table S1-2) and calculate the force-dependent event frequency, $k(f) = \sum N(f) / \sum t(f)$. We calculate the mean and standard error of k(f) by averaging values obtained from multiple groups.

The combined constant-velocity and constant-force data are fit with a log-linear relationship (**Figure 5**), in accordance with the simplest model of mechanochemical coupling (eq. 1).

$$\ln(k(f)) = C + \frac{F\Delta x^{\ddagger}}{RT} \tag{1}$$

As seen in Figure 5, the consensus data obtained by FC and CV measurements are well fit by eq. (1) across force-coupled rate constants from approximately 0.05 – 20 s⁻¹, with corresponding empirical mechanochemical coupling parameters, Δx^{\ddagger} , of 0.81 \pm 0.006 Å for CB3 and 1.46 ± 0.09 Å for **CB4**. Both Δx^{\ddagger} values obtained here are within experimental uncertainty of the approximated values derived from calculations previously reported by Boulatov and coworkers on similar cyclobutanes (~ 0.8 Å for diester "handles" and ~ 1.4 Å for diphenyl "handles"). The SMFS results therefore provide experimental support for the mechanism proposed therein, in which initial bond breaking to a diradical intermediate is the rate-limiting step of the net cycloreversion.¹³ In addition, the consistency within the FC and CV measurements indicates the success of the "binning" methodology in converting CV data into its FC equivalent.

A number of contributions go into the force dependency of reaction rate, most notably distortions of the reactant and transition state and the force-coupled change in length between the reactant and transition state. 45-47 The dependence changes with force, often in complicated ways that include contributions from multiple conformations, 48-49 as well as competing reaction paths and changes in mechanism that have been shown to be

relevant to the mechanical dissociation of cyclobutanes. ^{13,24} Nonetheless, given the similarity in the core reactant of both systems, the most likely contribution to the difference in the two systems is the better geometric coupling of the reaction path to the stretching force. In other words, the phenyl groups of **P4** act as metaphorical crowbars, ³⁶ relative to their alkyl counterparts in **P3**, allowing the applied force to be transmitted across a greater distance as the bond-breaking reaction proceeds.

Lastly, the reaction lengths determined here (~1 Å) are far smaller than the change in contour length expected for the formation of a fully open 1,4-diradicaloid intermediate or its subsequent disproportionation into alkenes. The empirical activation lengths are therefore consistent with a mechanistic picture in which the homolytic scission of the first bond is rate-determining at the forces examined here, as proposed by Boulatov. 13 Furthermore, the enhanced mechanical leverage provided by the phenyl group suggests that this scission event likely involve an increase in the torsional angle between the C-C bond that bridges the fused rings and the C-C bond connecting the cyclobutane to the pulling attachment. A given increase in bond length of the scissile carbon-carbon displaces the two pulling attachments to the same extent, but contributions from outwardly rotating attachments would be sensitive to the increased length of the phenyl "lever" relative to the methylene, as observed in electrocyclic reactions of alkene-substituted cyclopropanes.³⁶

Conclusion.

Cycloreversion releases an amount of stored length that is determined by the size of a fused macrocycle, and large unravelling events can be observed as single events in each of two different single molecule measurements. This allows us to characterize contour length changes associated with domain unravelling as well as details of the relative force dependencies. Here, the statistics of ring opening are well-described by models in which the mechanophores act as independent reactants with identical force-coupled reaction probabilities; reaction at one mechanophore does not detectably influence reactivity at another. The apparent independence of mechanophore reactivity need not be general, however, and approaches that permit stochastic events to be observed might prove useful in probing such systems. In addition, the dynamics of mechanically coupled tandem processes 14,25,50 are proving to be rich territory for mechanistic investigation, and with sufficient resolution single-event measurements might eventually be used to capture the force-coupled lifetimes and subsequent fate of reactive intermediates.

The differing reactivities of the two cyclobutane mechanophores arises from a combination of electronic and mechanical "lever arm" effects of the phenyl substituent relative to alkyl substituents. Similar effects have been observed in electrocyclic reactions, but we believe this to be the first experimental characterization of such an effect for a homolytic reaction. It suggests a torsional component to the mechanical scission reaction that need not be present in the force-free reaction. Regardless of the origin, the differences in reactivity make these cyclobutane promising candidates to help address fundamental questions of molecular extension, including the release of stored length, that accompanies the macroscopic stress-strain behavior of macroscopic polymer networks. We also note that, if the stored length were removed, these substituted cyclobutanes could be used as weak bonds with characterized scission behavior to probe the contributions of chain scission to polymers and polymer networks.

ASSOCIATED CONTENT

Supporting Information. Synthetic procedures, SMFS data collection and analysis. This material is available free of charge via the Internet at http://pubs.acs.org.

AUTHOR INFORMATION

Corresponding Authors

- *bdolsen@mit.edu
- *michael.rubinstein@duke.edu
- *stephen.craig@duke.edu

Author Contributions

‡These authors contributed equally.

ACKNOWLEDGMENT

This work was funded by Duke University and the Center for the Chemistry of Molecularly Optimized Networks (MONET), a National Science Foundation (NSF) Center for Chemical Innovation (CHE-1832256).

REFERENCES

- (1) Tskhovrebova, L.; Trinick, J.; Sleep, J. A.; Simmons, R. M. Elasticity and Unfolding of Single Molecules of the Giant Muscle Protein Titin. *Nature* **1997**, *387*, 308-312.
- (2) Rief, M.; Gautel, M.; Oesterhelt, F.; Fernandez, J. M.; Gaub, H. E. Reversible Unfolding of Individual Titin Immunoglobulin Domains by Afm. *Science* **1997**, *276*, 1109.
- (3) Oberhauser, A. F.; Hansma, P. K.; Carrion-Vazquez, M.; Fernandez, J. M. Stepwise Unfolding of Titin under Force-Clamp Atomic Force Microscopy. *Proc. Natl. Acad. Sci. U. S. A.* **2001**, *98*, 468-472.
- (4) Linke, W. A.; Grützner, A. Pulling Single Molecules of Titin by Afm—Recent Advances and Physiological Implications. *Pflügers Arch. Eur. J. Physiol.* **2008**, *456*, 101-115.
- (5) Chen, H.; Yuan, G.; Winardhi, R. S.; Yao, M.; Popa, I.; Fernandez, J. M.; Yan, J. Dynamics of Equilibrium Folding and Unfolding Transitions of Titin Immunoglobulin Domain under Constant Forces. *J. Am. Chem. Soc.* **2015**, *137*, 3540-3546.
- (6) Rivas-Pardo, Jaime A.; Eckels, Edward C.; Popa, I.; Kosuri, P.; Linke, Wolfgang A.; Fernández, Julio M. Work Done by Titin Protein Folding Assists Muscle Contraction. *Cell Rep.* **2016**, *14*, 1339-1347.
- (7) Eckels, E. C.; Tapia-Rojo, R.; Rivas-Pardo, J. A.; Fernández, J. M. The Work of Titin Protein Folding as a Major Driver in Muscle Contraction. *Annu. Rev. Physiol.* **2018**, *80*, 327-351.

- (8) Freundt, J. K.; Linke, W. A. Titin as a Force-Generating Muscle Protein under Regulatory Control. *J. Appl. Physiol.* **2018**, *126*, 1474-1482.
- (9) Guan, Z.; Roland, J. T.; Bai, J. Z.; Ma, S. X.; McIntire, T. M.; Nguyen, M. Modular Domain Structure: A Biomimetic Strategy for Advanced Polymeric Materials. *J. Am. Chem. Soc.* **2004**, *126*, 2058-2065
- (10) Fang, J.; Mehlich, A.; Koga, N.; Huang, J.; Koga, R.; Gao, X.; Hu, C.; Jin, C.; Rief, M.; Kast, J.; Baker, D.; Li, H. Forced Protein Unfolding Leads to Highly Elastic and Tough Protein Hydrogels. *Nat. Commun.* **2013**, *4*, 2974.
- (11) Chung, J.; Kushner, A. M.; Weisman, A. C.; Guan, Z. Direct Correlation of Single-Molecule Properties with Bulk Mechanical Performance for the Biomimetic Design of Polymers. *Nat. Mater.* **2014**, *13*, 1055-1062.
- (12) Bowser, B. H.; Ho, C. H.; Craig, S. L. High Mechanophore Content, Stress-Relieving Copolymers Synthesized Via Raft Polymerization. *Macromolecules* **2019**, *52*, 9032-9038.
- (13) Zhang, H.; Li, X.; Lin, Y.; Gao, F.; Tang, Z.; Su, P.; Zhang, W.; Xu, Y.; Weng, W.; Boulatov, R. Multi-Modal Mechanophores Based on Cinnamate Dimers. *Nat. Commun.* **2017**, *8*, 1147.
- (14) Tian, Y.; Cao, X.; Li, X.; Zhang, H.; Sun, C.-L.; Xu, Y.; Weng, W.; Zhang, W.; Boulatov, R. A Polymer with Mechanochemically Active Hidden Length. *J. Am. Chem. Soc.* **2020**, *142*, 18687-18697.
- (15) Levy, A.; Goldstein, H.; Brenman, D.; Diesendruck, C. E. Effect of Intramolecular Crosslinker Properties on the Mechanochemical Fragmentation of Covalently Folded Polymers. *J. Polym. Sci., Part A: Polym. Chem.* **2020**, *58*, 692-703.
- (16) Chen, Z.; Mercer, J. A. M.; Zhu, X.; Romaniuk, J. A. H.; Pfattner, R.; Cegelski, L.; Martinez, T. J.; Burns, N. Z.; Xia, Y. Mechanochemical Unzipping of Insulating Polyladderene to Semiconducting Polyacetylene. *Science* **2017**, *357*, 475.
 - (17) Craig, S. L. Up Another Rung. Nat. Chem. 2017, 9, 1154.
- (18) Wang, S.; Panyukov, S.; Rubinstein, M.; Craig, S. L. Quantitative Adjustment to the Molecular Energy Parameter in the Lake-Thomas Theory of Polymer Fracture Energy. *Macromolecules* **2019**, *52*, 2772-2777.
- (19) Pill, M. F.; Holz, K.; Preußke, N.; Berger, F.; Clausen-Schaumann, H.; Lüning, U.; Beyer, M. K. Mechanochemical Cycloreversion of Cyclobutane Observed at the Single Molecule Level. *Chem. Eur. J.* **2016**, *22*, 12034-12039.
- (20) Yang, J.; Horst, M.; Romaniuk, J. A. H.; Jin, Z.; Cegelski, L.; Xia, Y. Benzoladderene Mechanophores: Synthesis, Polymerization, and Mechanochemical Transformation. *J. Am. Chem. Soc.* **2019**, *141*, 6479-6483.
- (21) Li, M.; Zhang, H.; Gao, F.; Tang, Z.; Zeng, D.; Pan, Y.; Su, P.; Ruan, Y.; Xu, Y.; Weng, W. A Cyclic Cinnamate Dimer Mechanophore for Multimodal Stress Responsive and Mechanically Adaptable Polymeric Materials. *Polym. Chem.* **2019**, *10*, 905-910.
- (22) Kean, Z. S.; Black Ramirez, A. L.; Yan, Y.; Craig, S. L. Bicyclo[3.2.0]Heptane Mechanophores for the Non-Scissile and Photochemically Reversible Generation of Reactive Bis-Enones. *J. Am. Chem. Soc.* **2012**, *134*, 12939-12942.
- (23) Kean, Z. S.; Niu, Z.; Hewage, G. B.; Rheingold, A. L.; Craig, S. L. Stress-Responsive Polymers Containing Cyclobutane Core Mechanophores: Reactivity and Mechanistic Insights. *J. Am. Chem. Soc.* **2013**, *135*, 13598-13604.
- (24) Wang, J.; Kouznetsova, T. B.; Boulatov, R.; Craig, S. L. Mechanical Gating of a Mechanochemical Reaction Cascade. *Nat. Commun.* **2016**, *7*, 13433.
- (25) Chen, Z.; Zhu, X.; Yang, J.; Mercer, J. A. M.; Burns, N. Z.; Martinez, T. J.; Xia, Y. The Cascade Unzipping of Ladderane Reveals Dynamic Effects in Mechanochemistry. *Nat. Chem.* **2020**, *12*, 302-309.
- (26) Yang, J.; Horst, M.; Werby, S. H.; Cegelski, L.; Burns, N. Z.; Xia, Y. Bicyclohexene-Peri-Naphthalenes: Scalable Synthesis, Diverse Functionalization, Efficient Polymerization, and Facile Mechanoactivation of Their Polymers. *J. Am. Chem. Soc.* **2020**, *142*, 14619-14626.

- (27) Wu, D.; Lenhardt, J. M.; Black, A. L.; Akhremitchev, B. B.; Craig, S. L. Molecular Stress Relief through a Force-Induced Irreversible Extension in Polymer Contour Length. *J. Am. Chem. Soc.* **2010**, *132*, 15936-15938.
- (28) Wang, J.; Kouznetsova, T. B.; Niu, Z.; Ong, M. T.; Klukovich, H. M.; Rheingold, A. L.; Martinez, T. J.; Craig, S. L. Inducing and Quantifying Forbidden Reactivity with Single-Molecule Polymer Mechanochemistry. *Nat. Chem.* **2015**, *7*, 323-327.
- (29) Wang, S.; Beech, H. K.; Bowser, B. H.; Kouznetsova, T. B.; Olsen, B. D.; Rubinstein, M.; Craig, S. L. Mechanism Dictates Mechanics: A Molecular Substituent Effect in the Macroscopic Fracture of a Covalent Polymer Network. *J. Am. Chem. Soc.* **2021**, *143*, 3714-3718.
- (30) Lin, Y.; Kouznetsova, T. B.; Craig, S. L. Mechanically Gated Degradable Polymers. *J. Am. Chem. Soc.* **2020**, *142*, 2105-2109
- (31) Klukovich, H. M.; Kouznetsova, T. B.; Kean, Z. S.; Lenhardt, J. M.; Craig, S. L. A Backbone Lever-Arm Effect Enhances Polymer Mechanochemistry. *Nat. Chem.* **2013**, *5*, 110-114.
- (32) Lin, Y.; Kouznetsova, T. B.; Craig, S. L. A Latent Mechanoacid for Time-Stamped Mechanochromism and Chemical Signaling in Polymeric Materials. *J. Am. Chem. Soc.* **2020**, *142*, 99-103.
- (33) Barbee, M. H.; Kouznetsova, T.; Barrett, S. L.; Gossweiler, G. R.; Lin, Y.; Rastogi, S. K.; Brittain, W. J.; Craig, S. L. Substituent Effects and Mechanism in a Mechanochemical Reaction. *J. Am. Chem. Soc.* **2018**, *140*, 12746-12750.
- (34) Kouznetsova, T. B.; Wang, J.; Craig, S. L. Combined Constant-Force and Constant-Velocity Single-Molecule Force Spectroscopy of the Conrotatory Ring Opening Reaction of Benzocyclobutene. *ChemPhysChem* **2017**, *18*, 1486-1489.
- (35) Florin, E. L.; Rief, M.; Lehmann, H.; Ludwig, M.; Dornmair, C.; Moy, V. T.; Gaub, H. E. Sensing Specific Molecular Interactions with the Atomic Force Microscope. *Biosens. Bioelectron.* **1995**, *10*, 895-901
- (36) Wang, J.; Kouznetsova, T. B.; Kean, Z. S.; Fan, L.; Mar, B. D.; Martínez, T. J.; Craig, S. L. A Remote Stereochemical Lever Arm Effect in Polymer Mechanochemistry. *J. Am. Chem. Soc.* **2014**, *136*, 15162-15165.
- (37) Gossweiler, G. R.; Kouznetsova, T. B.; Craig, S. L. Force-Rate Characterization of Two Spiropyran-Based Molecular Force Probes. *J. Am. Chem. Soc.* **2015**, *137*, 6148-6151.
- (38) Wang, J.; Kouznetsova, T. B.; Niu, Z.; Rheingold, A. L.; Craig, S. L. Accelerating a Mechanically Driven Anti-Woodward-

- Hoffmann Ring Opening with a Polymer Lever Arm Effect. J. Org. Chem. 2015, 80, 11895-11898.
- (39) Zhang, Y.; Wang, Z.; Kouznetsova, T. B.; Sha, Y.; Xu, E.; Shannahan, L.; Fermen-Coker, M.; Lin, Y.; Tang, C.; Craig, S. L. Distal Conformational Locks on Ferrocene Mechanophores Guide Reaction Pathways for Increased Mechanochemical Reactivity. *Nat. Chem.* **2021**, *13*, 56-62.
- (40) Hioe, J.; Zipse, H. Radical Stability and Its Role in Synthesis and Catalysis. *Org. Biomol. Chem.* **2010**, *8*, 3609-3617.
- (41) Schlierf, M.; Li, H.; Fernandez, J. M. The Unfolding Kinetics of Ubiquitin Captured with Single-Molecule Force-Clamp Techniques. *Proc. Natl. Acad. Sci. U. S. A.* **2004**, *101*, 7299.
- (42) Hoffmann, T.; Dougan, L. Single Molecule Force Spectroscopy Using Polyproteins. *Chem. Soc. Rev.* **2012**, *41*, 4781-4796.
- (43) Serpe, M. J.; Kersey, F. R.; Whitehead, J. R.; Wilson, S. M.; Clark, R. L.; Craig, S. L. A Simple and Practical Spreadsheet-Based Method to Extract Single-Molecule Dissociation Kinetics from Variable Loading-Rate Force Spectroscopy Data. *J. Phys. Chem. C* **2008**, *112*, 19163-19167.
- (44) Oberbarnscheidt, L.; Janissen, R.; Oesterhelt, F. Direct and Model Free Calculation of Force-Dependent Dissociation Rates from Force Spectroscopic Data. *Biophys. J.* **2009**, *97*, L19-L21.
- (45) Huang, Z.; Boulatov, R. Chemomechanics: Chemical Kinetics for Multiscale Phenomena. Chem. Soc. Rev. 2011, 40, 2359-2384
- (46) Akbulatov, S.; Boulatov, R. Experimental Polymer Mechanochemistry and Its Interpretational Frameworks. *ChemPhysChem* **2017**, *18*, 1422-1450.
- (47) Tian, Y.; Boulatov, R. Comparison of the Predictive Performance of the Bell–Evans, Taylor-Expansion and Statistical-Mechanics Models of Mechanochemistry. *Chem. Commun.* **2013**, *49*, 4187-4189
- (48) Boulatov, R. The Challenges and Opportunities of Contemporary Polymer Mechanochemistry. *ChemPhysChem* **2017**, *18*, 1419-1421.
- (49) Akbulatov, S.; Tian, Y.; Huang, Z.; Kucharski, T. J.; Yang, Q.-Z.; Boulatov, R. Experimentally Realized Mechanochemistry Distinct from Force-Accelerated Scission of Loaded Bonds. *Science* **2017**, *357*, 299.
- (50) Nixon, R.; De Bo, G. Three Concomitant C–C Dissociation Pathways During the Mechanical Activation of an N-Heterocyclic Carbene Precursor. *Nat. Chem.* **2020**, *12*, 826-831.

